Compton Scattering with a ^{137}Cs source

Lei Katherine, Fortin Clément, Amar Selim

McGill University Department of Physics

Supervisor: Professor Dominic Ryan, Professor Peter Grütter

February 5, 2022

Abstract

Compton scattering is used to measure the rest mass energy of the electron. The radioactive sources ^{133}Ba, ^{57}Co, ^{22}Na and ^{137}Cs are used to calibrate our detector and a linear relationship between energy and channel of $E = m \cdot channel + b$ is found, with $m = 0.382(1)$ keV/channel and $b = -13.4(5)$ keV. Two values for the electron's rest mass energy are then determined using copper and aluminium scatterers: 510.4(50) keV [0.5 keV statistical and 5 keV systematic] and 532.6(20) keV [0.3 keV statistical and 2 keV systematic]. The first value is obtained by fitting the Compton equation in keV units while the second one is obtained by fitting it in channel units and then converting $m_e c^2$ into keV.

Contents

1 Apparatus and Calibration
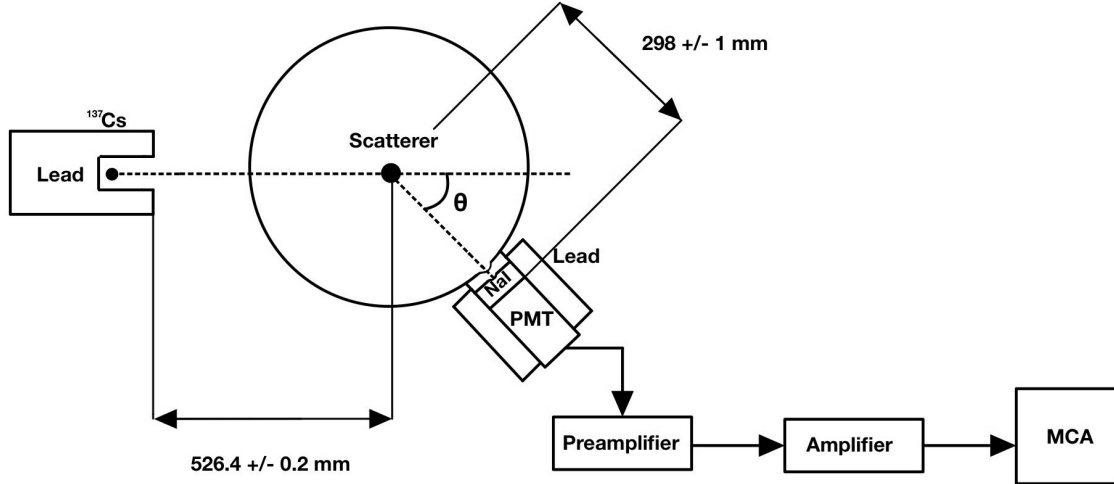
1.1 Equipment and Setup

Figure 1: A schematic diagram of the experimental arrangement for measuring the Compton scattering of ^{137}Cs gamma rays from scattering targets, comprising a ^{137}Cs source of 661.6 keV gamma rays, lead shields, interchangeable scattering rod, a detection circuit comprising a a NaI(Tl) scintillating crystal (Bicron [1]) on a rotating arm coupled to a photomultiplier tube (PMT)(Ortec 459 [2]) biased at V_{bias}, a preamplifier (Ortec 113 [3]), a pulseshaping amplifier (Canberra 816 [4]), and a multichannel analyzer (MCA, Ortec Easy-MCA-2k [5]). To do the calibration, radioactive sources are placed at the location of the scatterer and the strong ^{137}Cs source is blocked.

Figure 1 shows a schematic diagram of our apparatus used to measure the photons' energies. A NaI(Tl) scintillating crystal is positioned at an angle θ away from the line connecting the Cs-137 source and the scattering rod. When the gamma ray hits the crystal, it produces an amount of photons proportional to its energy. Some of them then come in contact with the active surface of the PMT and produce electrons through the photoelectric effect. The PMT amplifies these electrons into a discernible current pulse which is then converted to a voltage pulse by the preamplifier, and then further amplified and shaped by the amplifier. Finally, the MCA maps the peak voltage onto one of the 2048 channels available. As all the other previous processes are (approximatively) linear in their input, the MCA maps the peak voltage to a channel linearly in order for the relationship between energy and channel to come out (approximatively) linear. A zero-intercept is also used to

1

Finally, due to noise, the detected peaks are broaden into Gaussian distributions. This is caused by the light output from the crystal being spread over a time interval of about 10^{-6}sec. This results in the voltage peaks being spread out. By the central limit theorem, the means of these pulses (i.e. their channel) will then be normally distributed hence why we expect a Gaussian distribution. The right panel of Figure 2 shows the number of times each channel has been mapped to over a 30 seconds interval for a ^{57}Co source.
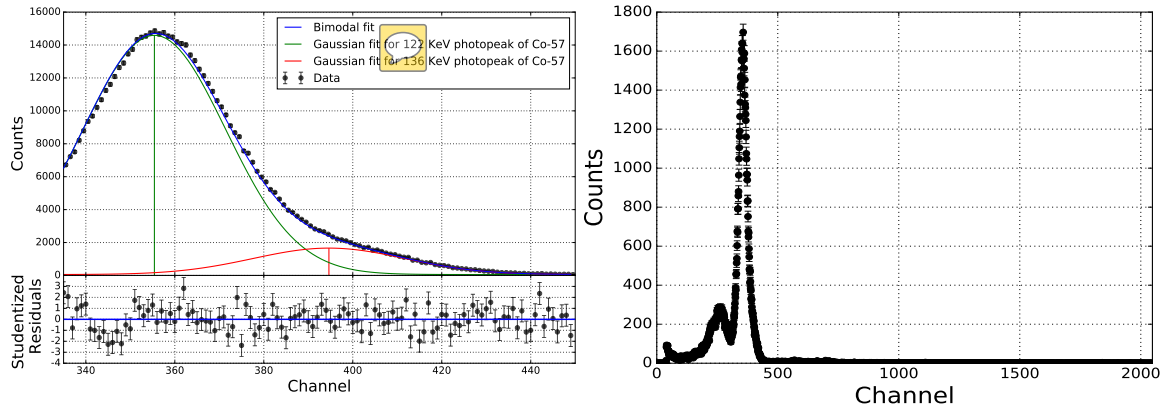
1.2 Calibration

Figure 2: Left: A bimodal distribution fitted against 5 minutes of ^{57}Co data with Poisson uncertainty. Right: 30 seconds time interval of data for ^{57}Co. The highest peak includes the two photopeaks while the smaller one on its left is of unknown origin and thus was not used in the calibration. The leftmost residuals in the bimodal fit exhibit structure due to the presence of this fictitious peak on their left.

To measure the scattered photons' energy, the relationship between energy and channel number need first be determined. This is done by collecting photon counts for four different sources with known gamma radiation [6–9]: ^{137}Cs, ^{133}Ba, ^{57}Co and ^{22}Na. To identify peak channels, Gaussian functions are fitted using least-square methods together with a background function. While for most a linear background function was enough to get rid of any structure in the residuals, the two peaks of ^{57}Co and the 31keV peak of ^{133}Ba required a bimodal fit (i.e., two Gaussians), as shown on the left panel of Figure 2, while the 302keV and 356keV peaks of ^{133}Ba were fitted using a trimodal fit. These multimodal fits allowed us

to use the small-intensity peaks of ^{57}Co at 136 keV and the one of ^{133}Ba at 302 keV in our calibration. The bimodal fit for ^{57}Co yields a reduced chi-squared of 1.2(1), indicating good agreement with the data and justifying the inclusion of the 136 keV peak. Similar statistical goodness was found for the other fits. Though other background functions have been tested, such as polynomials, they were seen to poorly fit the data under consideration. Further, statistical uncertainties are set assuming that the underlying distribution is Poisson, yielding an uncertainty of $\sqrt{N}$ on N counts.
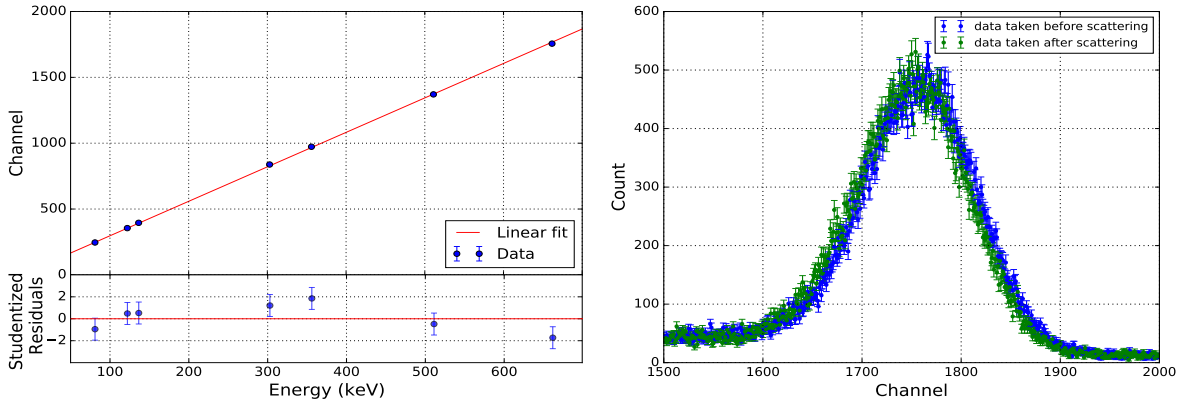

Figure 3: Left: Locations of 7 peak channels against their known energy. The fit parameters $m = 0.382(1)$ keV/channel and $b = -13.4(5)$ keV give the linear relationship $E = m \cdot ch + b$ with a reduced chi-squared of 1.5(6). The 31 keV peak of ^{133}Ba was omitted as it was seen to be an outlier. Right: Shift of the ^{137}Cs peak when using calibration data taken before or after scattering experiments. The shift is equal to 8 channels.

For each calibrating source, we plotted the peak channel number determined from the Gaussian fits against their corresponding energy values obtained from [6–9]. The statistical uncertainties in the peaks' locations were obtained from the Gaussian fits while three main sources of systematic uncertainties were identified. The first one was on the order of 0.5 channel and was estimated as the standard deviation of the distribution of peak locations we obtained when varying the channel region in which we were fitting. Furthermore, depending on which background function we used to model the noise, the location of the peak varied even though the corresponding fits had similar statistical goodness. The variation was on the order of 1 channel. The last source of systematic uncertainty is an observed shift in channel between calibration data taken before and after scattering measurements were done, as shown in Figure 3. Its contribution to the systematic uncertainty was estimated by fitting

3

Gaussian peaks using only the 'before' or 'after' data and then setting the extreme values as our upper and lower estimates. It varied between 0.5 to 4 channels for different sources. By fitting a linear function of the form of $y = x/m - b/m$ for channel against energy, we obtained the relationship $energy = m \times channel + b$ where $m = 0.382(1)$ keV/channel and $b = -13.4(5)$ keV, as shown in Figure 3. The reduced chi-squared of 1.5(6) indicates that the linear function is appropriate for describing the relationship between channel and energy. The 31 keV peak of ^{133}Ba was observed to be an outlier and was thus discarded.

2 Measurement of the Electron's Rest Mass Energy

The Compton equation expresses a photon's energy as a function of the scattering angle when scattered against a free electron:

$$E' = \frac{E}{1 + \frac{E}{m_e c^2}(1 + \cos\theta)}. \tag{1}$$

Where E' is the energy of the scattered photon, θ is the scattering angle, E is the initial energy of the ray and $m_e c^2$ is the rest mass energy of the electron. By fitting data to this equation, the latter can be extracted. Scattering and background data were taken for 6 angles on each side of the ^{137}Cs source. Both aluminium and copper rods were used in order to test whether the Compton equation depends on the material and to diminish any systematic uncertainties which we might introduce by using only one. At each angle, the background data is subtracted from the scattering data to remove the noise and the peak channel is found by fitting Gaussians. We find the same energy for the scattered photons and for $m_e c^2$ (within statistical uncertainties) for each material, therefore the Compton law doesn't depend on these material and it is justified to combine their data. Then, two methods were used to measure the rest mass energy of the electron. The first method consisted of converting the peak channel found at each angle into keV using our calibration, and then fitting Compton's equation to the resulting energy versus angle data shown in the left of Figure 4. The resulting rest mass energy of the electron with its statistical uncertainty is 510.4(3) keV. The systematic uncertainty is estimated by performing the fit with the lower

4

and upper lines of our calibration and setting the obtained values for $m_e c^2$, 505.8(3)keV and 515.2(3) keV, as our lower and upper estimates. The resulting systematic uncertainty is of 5 keV, giving us a measurement of $m_e c^2 = 510.4(50)$ keV. Even though the literature value of 511 keV lies within the range, the reduced chi-squared is 47.1(5) which suggests a poor fit. We then did the second method of plotting the peak channels directly against scattering angles as shown in the right of Figure 4. The Compton equation in unit of channels is fitted to the data and the electron rest mass energy is then converted to keV using our calibration, allowing for a clear distinction between systematic and statistical uncertainty. This fit gives a value and statistical uncertainty of $m_e c^2 = 532.6(3)$ keV. The systematic error is then simply given by $\sqrt{(m_{unc} * ch)^2 + b_{unc}^2}$ and is equal to 2 keV, which gives a measurement of $m_e c^2 = 532.6(20)$ keV. Even though the literature value does not fall within the range obtained with this second method, the statistical uncertainty and reduced chi-squares of 64.0(5) are on the same order as the first method. Therefore, we can not conclude which method gives a better result at the moment. This indicates that more data points is needed to obtain a more robust measurement, particularly at angles near 0° where the function varies the most.
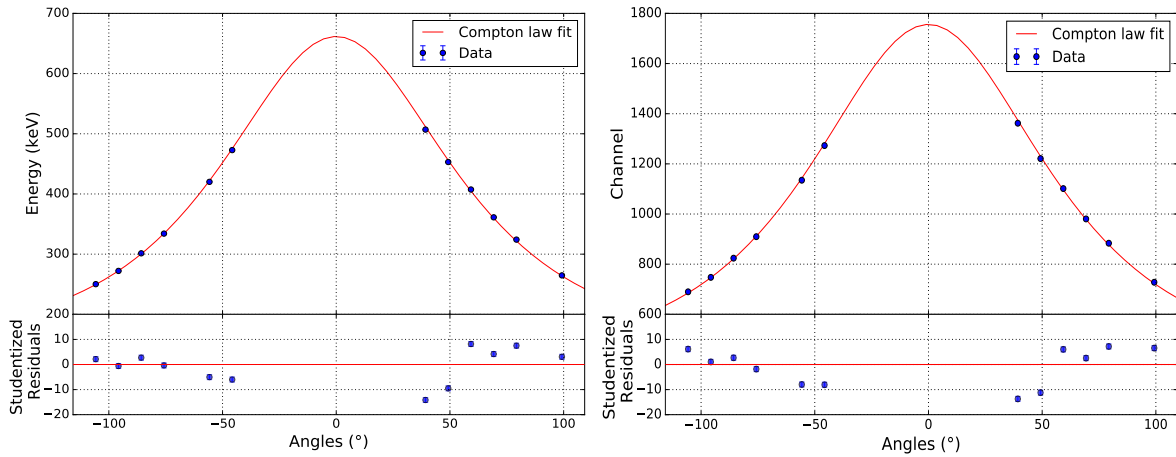

Figure 4: Left: Energy (keV) of the scattered photons versus the scattering angle with the Compton law fitted. It has a reduced chi-squared of 47.1(5) and gives a value of $m_e c^2 = 510.4(50)$keV. Right: Location of the photopeaks (channel) versus the scattering angle with the Compton law in units of channel fitted. The reduced chi-squared is 64.0(5) and it gives a value of $m_e c^2 = 532.6(20)$keV.

3 Comments, Progress and Future plans

3.1 Response to Comments

1. We made the abstract more concise and clearer.

2. We improved our calibration by 1) including the systematic error coming from the shift in peak channel from calibration data taken before and after the scattering measurement 2) including the systematic uncertainty from our choice of background function 3) removing the 31keV peak. The uncertainty in the slope of the calibration improved from 5% to 0.3% and the reduced chi-squared drops from 3415.8(6) to 1.5(6).

3. We clearly specified different sources of systematic uncertainty for each quantities and how their effect was estimated. We also made the distinction between statistical and systematic uncertainties in all our measurements in order to express how the later affects our results.

4. We gave a more in-dept explanation of how the apparatus works and explained what causes the noise that broadens the peaks and why it's Gaussian.

5. Fixed typos in subsection 1.1, added scale in schematic diagram, described why the MCA maps the peak voltage to channel linearly.

6. Made the font bigger in our plots and made them all of the same style (with legends for each of them).

7. We worked in original units for our fit of the Compton equation in order not to mess up the uncertainty.

3.2 Other Attempts and Progress

1. We tried fixing some parameters in the Compton equation to fixed values versus letting them as free parameters to see how much the rest mass energy changes. This didn't make the two estimates for $m_e c^2$ closer and didn't improve the fits. We also tried to include a constant offset to the channel versus angle fit but once again no improvement was found.

2. We asked for additional data on angles closer to 0 degrees since we observed that the poorness of both fits were most likely due to the lack of data in the middle region of the plot. We also asked for data on both sides of the source and saw an improvement in our fits.

3. We fitted for the "direct" angle as a parameter instead of assuming it to be 180 degrees.

4. We noticed and fixed an error we made when computing the uncertainty on the counts with subtracted "no scatterer" data.

3.3 Future Plans

1. Acquiring scattering data near 0° in order to improve our fits for both energy versus angle and channel versus angle. This includes getting additional data for the 125°, 135°, 220° and 230° angles as the fits are the most sensible to these points. We also want to obtain data for angles closer to 0° as we've been informed that additional angles will be measured soon.

2. We also plan on taking into account the efficiency of the detector in order to see if that has any effects on our two fits. Indeed, the efficiency varies with energy hence can deform our peaks and potentially affect their mean.

3. We then want to move on to comparing the Thomson and Klein-Nishina predictions for the cross section by fitting the two equations and seeing which fit best captures the behaviour of the data.

References

[1] S.-G. Crystals. (2005) NaI(TI) and Polyscin® NaI(TI) Sodium Iodide Scintillation Material. [Online]. Available: https://www.crystals.saint-gobain.com/sites/hps-mac3-cma-crystals/files/2021-08/Sodium-Iodide-Material-Data-Sheet.pdf 1

[2] Ortec. (2002) 266 Photomultiplier Base. [Online]. Available: https://www.ortec-online.com/products/electronics/photomultiplier-tube-bases/266 1

[3] Ortec. (2002) 113 Scintillation Preamplifier. [Online]. Available: https://www.ortec-online.com/products/electronics/preamplifiers/113 1

[4] Canberra. Spectroscopy Amplifier Model 816. [Online]. Available: http://www.nuclearphysicslab.com/npl/wp-content/uploads/Canberra_816_Spectroscopy_Amplifier.pdf 1

[5] Ortec. (2014) Easy-MCA 2k or 8k Channel Multichannel Analyzer. [Online]. Available: https://www.ortec-online.com/products/electronics/multichannel-analyzers-mca/basic-analog/easy-mca-2k-or-8k 1

[6] Y. Khazov, A. Rodionov, and F. Kondev, "Nuclear Data Sheets for A = 133," *Nuclear Data Sheets*, vol. 112, no. 4, pp. 855–1113, 2011. [Online]. Available: https://www.sciencedirect.com/science/article/pii/S0090375211000202 2, 3

[7] M. R. Bhat, "Nuclear Data Sheets for A = 57," *Nucl. Data Sheets*, vol. 85, pp. 415–536, 1998. [Online]. Available: https://www.sciencedirect.com/science/article/abs/pii/S0090375298900217?via%3Dihub 2, 3

[8] E. Browne and J. Tuli, "Nuclear Data Sheets for A = 137," *Nuclear Data Sheets*, vol. 108, no. 10, pp. 2173–2318, 2007. [Online]. Available: https://www.sciencedirect.com/science/article/pii/S0090375207000804 2, 3

[9] M. S. Basunia, "Nuclear Data Sheets for A = 22," *Nuclear Data Sheets*, vol. 127, pp. 69–190, 2015. [Online]. Available: https://www.sciencedirect.com/science/article/pii/S0090375215000253 2, 3